Microfluid Nanofluid (2011) 11:105–110
DOI 10.1007/s10404-011-0785-6

SHORT COMMUNICATION

Sedimentation pinched-flow fractionation for size- and density-based particle sorting in microchannels

Tomoki Morijiri · Satoshi Sunahiro · Masashi Senaha · Masumi Yamada · Minoru Seki

Received: 3 November 2010 / Accepted: 1 February 2011 / Published online: 8 March 2011

Abstract A simple and efficient device for density-based particle sorting is in high demand for the purification of specific cells, bacterium, or environmental particles for medical, biochemical, and industrial applications. Here we present microfluidic systems to achieve size- and density-based particle separation by adopting the sedimentation effect for a size-based particle sorting technique utilizing microscale hydrodynamics, called "pinched-flow fractionation (PFF)." Two schemes are presented: (a) the particle inertia scheme, which utilizes the inertial force of particle movement induced by the momentum change in the curved microchannel, and (b) the device rotation scheme, in which rotation of the microdevice exerts centrifugal force on the flowing particles. In the experiments, we successfully demonstrated continuous sorting of microparticles according to size and density by using these two schemes, and showed that the observed particle movements were in good agreement with the theoretical estimations. The presented schemes could potentially become one of the functional components for integrated bioanalysis systems that can manipulate/separate small amount of precious biological samples.

Electronic supplementary material The online version of this article (doi:10.1007/s10404-011-0785-6) contains supplementary material, which is available to authorized users.

T. Morijiri · S. Sunahiro · M. Senaha · M. Yamada · M. Seki (✉)
Department of Applied Chemistry and Biotechnology, Chiba University, 1-33 Yayoi-cho, Inage-ku, Chiba 263-8522, Japan
e-mail: mseki@faculty.chiba-u.jp

S. Sunahiro
Department of Chemical Engineering, Osaka Prefecture University, 1-1 Gakuen-cho Naka-ku, Sakai, Osaka 599-8531, Japan

Keywords Particle separation · Pinched-flow fractionation · Inertial microfluidics · Centrifugal microfluidics · Density

Abbreviation
PFF Pinched-flow fractionation

1 Introduction

Separation of particulate samples according to density is often a crucial step in chemical and biological preparations. For instance, white blood cells are routinely classified into sub-populations by employing density-gradient centrifugation in clinics and biomedical laboratories (English and Andersen 1974). Density is also often used to distinguish stem cells (Broxmeyer et al. 1989; Rambaldi et al. 1998; Jones et al. 1990), dead/alive cells (Yamada and Ohyama 1980; Lindqvist et al. 1997), and specific bacterium in a complex mixture (Chesnot and Schwartzbrod 2004).

To date, a number of researchers have demonstrated continuous particle separation in lab-on-a-chip devices (Pamme 2007). Some of them utilize a stably formed laminar flow (Yamada et al. 2004; Takagi et al. 2005; Yamada and Seki 2005; Jäggi et al. 2007; Sethu et al. 2006; Huang et al. 2004), while others additionally make use of Dean flows in curved channels (Bhagat et al. 2008; Kuntaegowdanahalli et al. 2009; Yoon et al. 2009), inertial lift force (Di Carlo et al. 2007), acoustic pressure (Nilsson et al. 2004; Petersson et al. 2005), electric fields (Doh and Cho 2005), magnetic fields (Pamme and Wilhelm 2006), gravity (Huh et al. 2007), or centrifugal force (Haeberle et al. 2006). Although these studies have proved the

versatility and applicability of microfluidics for precise handling of micrometer-sized samples, only a few works have achieved density-based particle separation in microchannels (Petersson et al. 2005; Huh et al. 2007; Haeberle et al. 2006), just showing particle sorting into only two subfractions or extraction of fluids from suspensions. Centrifugal SPLITT fractionation (Fuh et al. 1994) is a conventional technique to achieve continuous particle sorting into multiple fractions based on the sedimentation velocity, using a large-scale rotating column equipped with multiple external pumps. A microfluidic technique for easily achieving density-based cell/particle fractionation would be highly useful as an essential unit operation in integrated microdevices for biological applications.

In this short communication, we present simple and unique systems to achieve continuous size- and density-based separation of particles, by employing the sedimentation effect and the previously developed pinched-flow fractionation (PFF) technique (Yamada et al. 2004; Takagi et al. 2005). The concept of sedimentation PFF is shown in Fig. 1. The microfluidic channel consists of two inlet channels, a relatively narrow junction (pinched segment) and a curved channel equipped with multiple outlet channels. Fluid flows with and without particles are, respectively, introduced from each inlet channel. Particles are initially focused onto one sidewall of the pinched segment, creating a difference in particle center positions according to size. This difference is then amplified in the broadened and curved channel downstream, with the particles being separated based on size. Here in the curved channel, the sedimentation force is exerted perpendicularly to the primary flow to move the particles outward. Consequently, particles with a higher density move more toward the outer side than particles with the same size but lower density, recovering the former from the upstream outlet channels.

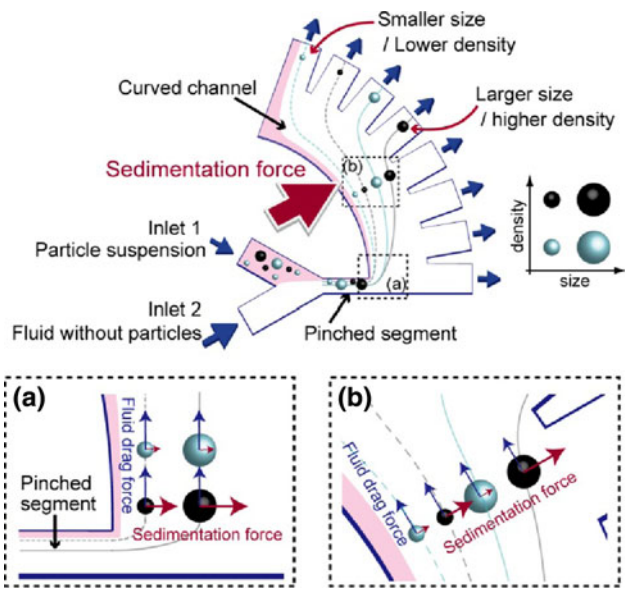

Fig. 1 Schematic illustrations showing the separation mechanism of sedimentation pinched-flow fractionation. Images **a** and **b** show enlarged views of areas (*a*) and (*b*) of the upper image, respectively. In the pinched segment, particles are focused onto the upper sidewall regardless of size. By applying sedimentation force to the flowing particles in the curved channel, particles with a higher density (*black*) migrate beyond the streamline, achieving density-based sorting

We propose and compare two schemes to exert the sedimentation force in the curved channel: (a) the particle inertia scheme and (b) the device rotation scheme. In (a), pressure-driven flow is employed to transport fluids and particles, and the momentum change in the curved channel with a relatively small radius induces the inertial force to move the particles outward. While in (b), the rotation of the microdevice generates both the sedimentation effect and the driving force to transport fluids through the microchannel.

2 Experimental setup

Microfluidic devices were fabricated using standard soft lithography and replica molding techniques. PDMS prepolymer (SILPOT 184, Dow Corning Toray Corp., Japan) was poured on a silicon mold having patterned SU-8 structures (SU-8 2010, Microchem Corp., USA) and cured to obtain a PDMS replica. The replica was irreversibly bonded with a flat PDMS plate by O_2-plasma oxidation using a plasma reactor (PR500, Yamato Scientific Corp., Japan).

The designs of the PDMS microdevices are shown in Fig. 2. Both devices have two inlet and 12 outlet channels. In the microdevice for the particle inertia scheme (Fig. 2a), the radius of the curved channel is relatively small, 1 mm, to effectively generate the inertial force. In contrast, the curvature radius in the microdevice for the device rotation scheme (Fig. 2b) must be relatively large (15 mm), to apply a strong centrifugal force and achieve a long retention time. Also in Device (b), the hydrodynamic resistances and the positions of the inlet channels were properly adjusted in order to control the inlet flow rates; the theoretical ratio of the volumetric flow rates from Inlets 1 and 2 is 1:20, where particles larger than $\sim$1.5 μm are expected to be focused onto the upper sidewall in the pinched segment. The theoretical estimation of the volumetric flow rate distributed to each outlet is shown in Table S1 in Electronic Supplementary Material.

Fluorescent polystyrene microbeads, with a diameter of either 3.0 or 5.0 μm ($\rho = 1.05$ g cm^{-3}; R0300 and G0500, Duke Scientific Corp., CA, USA) and non-fluorescent silica microspheres with an average diameter of 5.0 μm ($\rho = 2.0$ g cm^{-3}; Polysciences Inc., PA, USA) were suspended in 0.5% (w/v) Tween 80 aqueous solution ($\rho = 1.00$ g cm^{-3}).

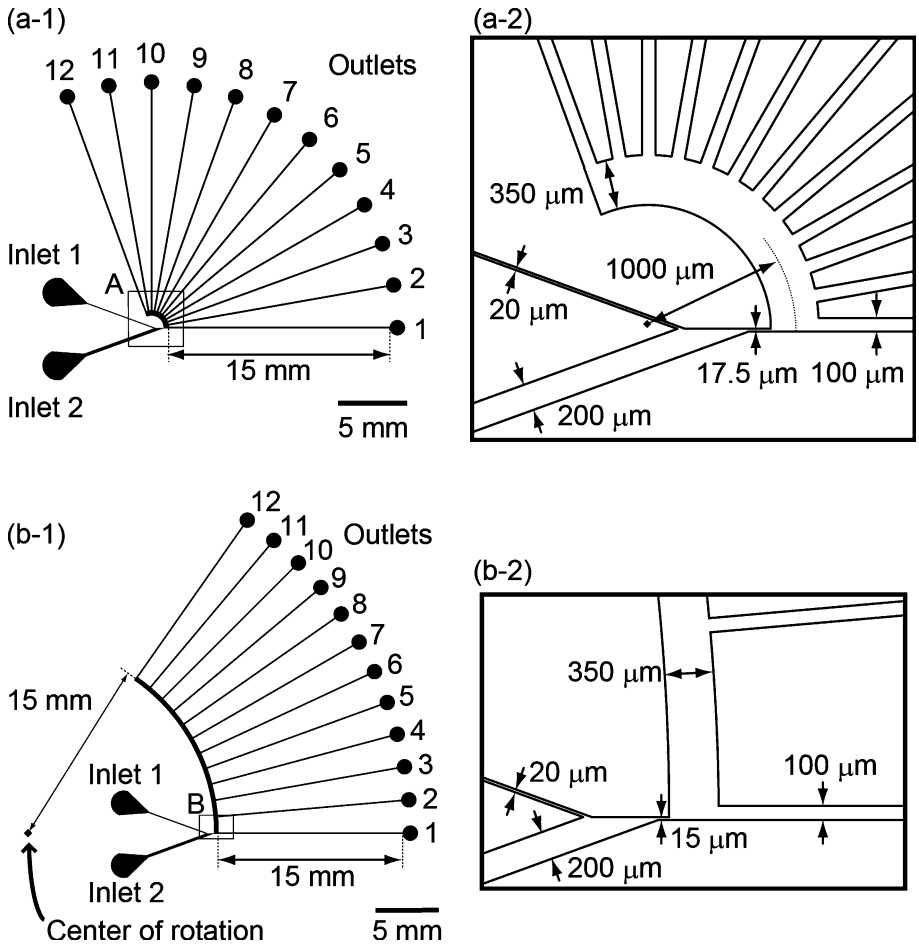

Fig. 2 Schematic diagrams showing microchannel designs; whole microchannel designs and enlarged views of the junction area *A* and *B* for **a** particle inertia and **b** device rotation schemes, respectively. Channel depth is uniform for both devices, 10 μm

The concentrations of these particles were 6.7×10^5, 1.5×10^5, and 1.1×10^5 particles per 1 μl, respectively. In the particle inertia scheme, the device was treated with O_2 plasma just before conducting the experiments to render the inner surface of the microchannel hydrophilic. The solutions with and without particles were introduced into the microchannel using syringe pumps (KD Scientific Corp., USA) at a fixed ratio of inlet volumetric flow rates, 3:100. The separation behavior of the particles was observed by using a fluorescence microscope (IX-71, Olympus Corp., Japan), and the particles flowing through each outlet branch channel were counted.

In the device rotation scheme, the microdevice was treated with O_2 plasma and the entire microchannel was filled with buffer solution containing no particles. Each inlet and outlet port was then partially covered by a lid of thin PDMS membrane in order to prevent the solutions from spilling out of the inlet/outlet ports during device rotation. The solution in Inlet port 1 was then replaced with the particle suspension, and the device was rotated on a spinning device (1H-D7, MIKASA Corp., Japan) for 30, 150, and 300 s when the rotation speeds were 3000, 1500, and 750 rpm, respectively. After finishing the rotation, the particles in each outlet were counted under the microscope.

3 Results and discussion

3.1 Particle sorting based on the particle inertia scheme

For the particle inertia scheme, we put a simple estimation of the sedimentation effect on particles in the curved channel. The sedimentation velocity of particles caused by the inertial force due to the momentum change, U_s, is expressed by the following equation (Park and Jung 2009):

$$U_s = \frac{\rho_p}{18 r_c \mu} D_p^2 U^2 \quad (1)$$

where ρ_p is the particle density, D_p is the particle diameter, U is the average flow velocity, r_c is the curvature radius of the flow, and μ is the fluid viscosity. Equation 1 shows that the sedimentation velocity, U_s, is proportional to the square of the flow rate (U^2). Since the retention time, τ, is inversely proportional to the flow rate (U), and

the migration distance is given as a product of τ and U_s, it was expected that a higher flow rate would result in a greater migration distance and a shift of the outlet of particle recovery to the upstream one (outlet with a smaller number).

Figure 3a-1 shows micrographs of the flowing polystyrene and silica particles near the end of the curved channel when the total flow rate was changed as indicated. The increase in the flow rate clearly resulted in a significant amplification of the distance between the trajectories of these particles. As shown in Fig. 3a-2, the recovery positions of particles gradually shifted to the upstream outlets (outlets with the smaller numbers) with an increase in the flow rate due to the larger migration distance under the higher flow-rate conditions, which is suggested from Eq. 1. Under a relatively low-flow rate condition (515 μl h^{-1}), particles were separated solely based on size, as in the case of the conventional PFF where the sedimentation effect was not considered. When the flow rate was increased to 2060 μl h^{-1}, we were able to sort these three types of particles continuously based on both size and density. However, when the flow rate was as high as 3090 μl h^{-1}, dispersions in the particle positions were significant; 5.0 μm silica and polystyrene particles flowed through the downstream outlets compared to the 2060 μl h^{-1} condition, suggesting that these particles moved toward the inner sidewall against the sedimentation force. A possible reason for this dispersion is the presence of a secondary flow called the Dean flow (Bhagat et al. 2008; Kuntaegowdanahalli et al. 2009; Yoon et al. 2009), which is usually observed in a curved channel under relatively high flow-rate conditions, and which would hinder the sedimentation effect caused by the inertial force of particle movement. In this sense, we were able to fully exploit the sedimentation effect at a flow rate of 2060 μl h^{-1}, without being affected by the Dean flows.

3.2 Particle sorting based on the device rotation scheme

To improve the resolution of density-based separation, the second scheme was proposed that employs the centrifugal force generated by device rotation. In this scheme, both the sedimentation-based particle separation and the fluid pumping are conducted by the device rotation. Here we also made a simple estimation of the sedimentation effect on particle movement. The sedimentation velocity U_s' is determined by both the inertial and centrifugal effects, and expressed as follows:

$$U_s' = U_s + U_c = \frac{\rho_p}{18 r_c \mu} D_p^2 U^2 + \frac{\rho_p - \rho_f}{18\mu} D_p^2 r_d \omega^2 \quad (2)$$

where U_c is the migration velocity caused by the centrifugal force, r_d is the distance between the particle and the center of rotation, ρ_f is the fluid density, and ω is the angular velocity of device rotation. Due to the relatively large curvature radius and the low flow rate driven by the device rotation, the sedimentation effect caused by the inertial force U_s is negligible in Device (b). Equation 2 indicates that the sedimentation velocity U_s' is proportional to the square of the angular velocity. Since the retention time, τ, is inversely proportional to the square of the angular velocity, ω, as shown in Eq. S16 of the Electronic Supplementary Material, and the migration distance is

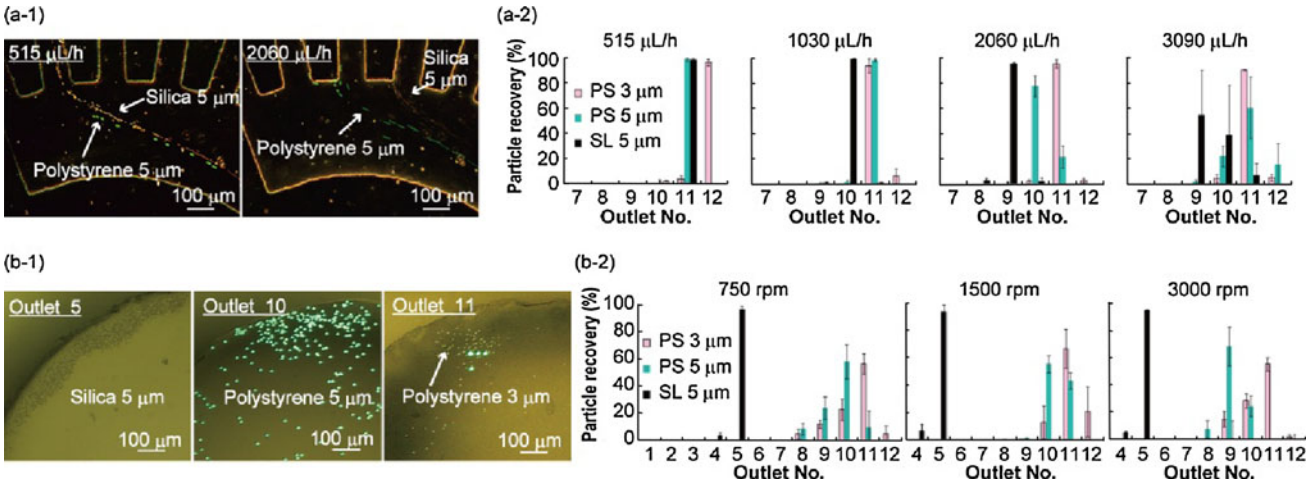

Fig. 3 Separation results in **a** particle inertia and **b** device rotation schemes. **a-1** Micrographs showing the flowing 5.0 μm silica and polystyrene particles, and **a-2** recovery rates of particles from each outlet, when the total flow rate was changed as indicated. In **a-1**, multiple images were superimposed. **b-1** Micrographs of outlets after rotating at 750 rpm for 300 s, and **b-2** recovery rates of particles. Each data bar in **a-2** and **b-2** represents the mean ± SD from at least three independent experiments. *PS* polystyrene and *SL* silica particles

Table 1 Theoretical and experimental outlets of 3.0 μm polystyrene (PS3), 5.0 μm polystyrene (PS5), and 5.0 μm silica (SL5) particles in (a) the particle inertia scheme

Volumetric flow rate	515 μl h^{-1}			1030 μl h^{-1}			2060 μl h^{-1}			3090 μl h^{-1}		
Particles	PS3	PS5	SL5	PS3	PS5	SL5	PS3	PS5	SL5	PS3	PS5	SL5
Theoretical outlet	11	11	11	11	11	11	11	11	10	11	11	10
Experimental outlet	12	11	11	11	11	10	11	10	9	11	11	9

Table 2 Theoretical and experimental outlets of 3.0 μm polystyrene (PS3), 5.0 μm polystyrene (PS5), and 5.0 μm silica (SL5) particles in (b) the device rotation scheme

Rotation speed	750 rpm			1500 rpm			3000 rpm		
Particles	PS3	PS5	SL5	PS3	PS5	SL5	PS3	PS5	SL5
Theoretical outlet	11	9	4	11	9	4	11	9	4
Experimental outlet	11	10	5	11	10	5	11	9	5

given as a product of U_s' and τ, it was expected that the flowing positions of particles and the outlets of particle recovery would be independent of the rotation speed.

Figure 3b-1 shows photographs of the separated particles in Outlets 5, 10, and 11, when the microdevice was rotated at 750 rpm for 300 s. The ratios of particle recovery from each outlet, when the rotation speeds were 750, 1500, and 3000 rpm, respectively, are shown in Fig. 3b-2. Under these conditions, most of the silica particles flowed through Outlet 5, showing that the influence of the rotation speed on the separation efficiency was not highly significant, and the robustness of the scheme against the operation conditions. It should be noted that the average Dean numbers of this scheme (0.0009–0.01) were significantly lower than those of the particle inertia scheme (0.07–0.4), which resulted in a lesser influence of the Dean flows with a higher separation efficiency compared to the particle inertia scheme. Although the throughput would be not as that of the particle inertia scheme, this scheme is advantageous since the operation process does not require external pumps, while it achieves more efficient density-based particle separation.

3.3 Modeling of the particle behaviors

To predict and validate the outlets of particle recovery, we made theoretical estimations of the behaviors of 3.0 μm polystyrene, 5.0 μm polystyrene, and 5.0 μm silica particles for both particle inertia and device rotation schemes. The outlets would be predictable by considering (1) the initial positions of the particles at the entrance of the curved channel, (2) the lateral migration velocity of particles caused by the particle inertia and/or device rotation, and (3) the fluid drainage through each outlet, which determines the flow profile in the curved channel and the retention times of the particles. In order to simplify the theoretical estimation, we separated the curved channel into 12 zones, neglected the parabolic flow-rate distribution, and simplified the particle trajectories as shown in Electric Supplemental Materials. Based on the estimations, the theoretical outlets of 3.0 μm polystyrene, 5.0 μm polystyrene, and 5.0 μm silica particles were calculated, and they were compared with the experimental results as shown in Tables 1 and 2, where the experimental results represent the number of the outlet where the ratio of the recovered particles was maximum. We confirmed that the theoretical values corresponded well with the experimental results, although there are dispersions in the experimental results (Fig. 3a-2, b-2), and slight differences between the theoretical and experimental values.

4 Conclusions

We successfully combined the PFF technique and the sedimentation effect to achieve density-based continuous sorting of particles. Two schemes were proposed and examined; the particle inertia scheme was advantageous in terms of throughput and simplicity in operation, while the device rotation scheme showed better separation efficiency. Although the effects of density and size are not completely separate, the presented schemes could have great potential as one of the essential microfluidic components for lab-on-a-chip systems and integrated bioanalysis devices.

Acknowledgments This study was supported in part by Grants-in-aid for Scientific Research A (20241031) from Ministry of Education, Culture, Science, and Technology (MEXT), Japan, and for Improvement of Research Environment for Young Researchers from Japan Science and Technology Agency.

References

Bhagat AAS, Kuntaegowdanahalli SS, Papautsky I (2008) Continuous particle separation in spiral microchannels using dean flows and differential migration. Lab Chip 8:1906–1914. doi:10.1039/b807107a

Broxmeyer HE, Douglas GW, Hangoc G, Cooper S, Bard J, English D, Arny M, Thomas L, Boyse EA (1989) Human umbilical cord

blood as a potential source of transplantable hematopoietic stem/progenitor cells. Proc Natl Acad Sci USA 86:3828–3832

Chesnot T, Schwartzbrod J (2004) Quantitative and qualitative comparison of density-based purification methods for detection of *Cryptosporidium* oocysts in turbid environmental matrices. J Microbiol Methods 58:375–386. doi:10.1016/j.mimet.2004.05.001

Di Carlo D, Irimia D, Tompkins RG, Toner M (2007) Continuous inertial focusing, ordering, and separation of particles in microchannels. Proc Natl Acad Sci USA 104:18892–18897. doi:10.1073/pnas.0704958104

Doh I, Cho YH (2005) A continuous cell separation chip using hydrodynamic dielectrophoresis (DEP) process. Sens Actuators A 121:59–65. doi:10.1016/j.sna.2005.01.030

English D, Andersen BR (1974) Single-step separation of red blood cells. Granulocytes and mononuclear leukocytes on discontinuous density gradients of Ficoll-Hypaque. J Immunol Methods 5:249–252. doi:10.1016/0022-1759(74)90109-4

Fuh CB, Myers MN, Giddings JC (1994) Centrifugal SPLITT fractionation: new technique for separation of colloidal particles. Ind Eng Chem Res 33:355–362

Haeberle S, Brenner T, Zengerle R, Ducrée J (2006) Centrifugal extraction of plasma from whole blood on a rotating disk. Lab Chip 6:776–781. doi:10.1039/b604145k

Huang LR, Cox EC, Austin RH, Sturm JC (2004) Continuous particle separation through deterministic lateral displacement. Science 304:987–990. doi:10.1126/science.1094567

Huh D, Bahng JH, Ling Y, Wei HH, Kripfgans OD, Fowlkes JB, Grotberg JB, Takayama S (2007) Gravity-driven microfluidic particle sorting device with hydrodynamic separation amplification. Anal Chem 79:1369–1376. doi:10.1021/ac061542n

Jäggi RD, Sandoz R, Effenhauser CS (2007) Microfluidic depletion of red blood cells from whole blood in high-aspect-ratio microchannels. Microfluid Nanofluid 3:47–53. doi:10.1007/s10404-006-0104-9

Jones RJ, Wagner JE, Celano P, Zicha MS, Sharkis SJ (1990) Separation of pluripotent haematopoietic stem cells from spleen colony-forming cells. Nature 347:188–189. doi:10.1038/347188a0

Kuntaegowdanahalli SS, Bhagat AAS, Kumar G, Papautsky I (2009) Inertial microfluidics for continuous particle separation in spiral microchannels. Lab Chip 9:2973–2980. doi:10.1039/B908271A

Lindqvist R, Norling B, Lambertz ST (1997) A rapid sample preparation method for PCR detection of food pathogens based on buoyant density centrifugation. Lett Appl Microbiol 24:306–310

Nilsson A, Petersson F, Jönsson H, Laurell T (2004) Acoustic control of suspended particles in micro fluidic chips. Lab Chip 4:131–135. doi:10.1039/b313493h

Pamme N (2007) Continuous flow separations in microfluidic devices. Lab Chip 7:1644–1659. doi:10.1039/b712784g

Pamme N, Wilhelm C (2006) Continuous sorting of magnetic cells via on-chip free-flow magnetophoresis. Lab Chip 6:974–980. doi:10.1039/b604542a

Park JS, Jung H (2009) Multiorifice flow fractionation: continuous size-based separation of microspheres using a series of contraction/expansion microchannels. Anal Chem 81:8280–8288. doi:10.1021/ac9005765

Petersson F, Nilsson A, Holm C, Jönsson H, Laurell T (2005) Continuous separation of lipid particles from erythrocytes by means of laminar flow and acoustic standing wave forces. Lab Chip 5:20–22. doi:10.1039/b405748c

Rambaldi A, Borleri G, Dotti G, Bellavita P, Amaru R, Biondi A, Barbui T (1998) Innovative two-step negative selection of granulocyte colony-stimulating factor-mobilized circulating progenitor cells: adequacy for autologous and allogeneic transplantation. Blood 91:2189–2196

Sethu P, Sin A, Toner M (2006) Microfluidic diffusive filter for apheresis (leukapheresis). Lab Chip 6:83–89. doi:10.1039/b512049g

Takagi J, Yamada M, Yasuda M, Seki M (2005) Continuous particle separation in a microchannel having asymmetrically arranged multiple branches. Lab Chip 5:778–784. doi:10.1039/b501885d

Yamada T, Ohyama H (1980) Separation of the dead cell fraction from X-irradiated rat thymocyte suspensions by density gradient centrifugation. Int J Radiat Biol 37:695–699

Yamada M, Seki M (2005) Hydrodynamic filtration for on-chip particle concentration and classification utilizing microfluidics. Lab Chip 5:1233–1239. doi:10.1039/b509386d

Yamada M, Nakashima M, Seki M (2004) Pinched flow fractionation: continuous size separation of particles utilizing a laminar flow profile in a pinched microchannel. Anal Chem 76:5465–5471. doi:10.1021/ac049863r

Yoon DH, Ha JB, Bahk YK, Arakawa T, Shoji S, Go JS (2009) Size-selective separation of micro beads by utilizing secondary flow in a curved rectangular microchannel. Lab Chip 9:87–90. doi:10.1039/b809123d